PHYSICAL REVIEW D **75,** 014027 (2007)

Test of the reaction mechanism for $\gamma N \to K\Lambda(1520)$ using the polarized photon

Seung-il Nam,[1,*] Ki-Seok Choi,[1,†] Atsushi Hosaka,[2,‡] and Hyun-Chul Kim[1,§]

[1]*Department of Physics and Nuclear Physics & Radiation Technology Institute (NuRI), Pusan National University, Busan 609-735, Korea*

[2]*Research Center for Nuclear Physics (RCNP), Ibaraki, Osaka 567-0047, Japan*

(Received 16 November 2006; published 30 January 2007)

We study the reaction mechanism for the photoproduction of the $\Lambda(1520)$, based on an effective Lagrangian approach. We investigate each contribution of the s-, u-, t-channel processes and contact term, separately. One of the most characteristic features of this reaction is the contact-term dominance which governs the photoproduction from the proton, when the K^*-exchange contribution is possibly not too large. We suggest several different ways of the polarizations and arrangement of the beam and target to understand the role of each contribution separately in future experiments.

DOI: 10.1103/PhysRevD.75.014027 PACS numbers: 13.75.Cs, 14.20.−c

I. INTRODUCTION

Recent activities in hadron physics are largely motivated by the observation signals for exotic hadrons. Perhaps one of the most influential ones is the Θ^+. After a great amount of effort, we are now at the stage of more careful investigation on the matter. The study of the exotic hadrons, at the same time, has brought revised interest in the physics of hadron resonances in general. Among them, of particular interest is the sector of strangeness $S = -1$. The properties of the $\Lambda(1405)$ as well as the $\bar{K}$–N interaction have been discussed in many different ways; one noticeable suggestion was made for the $\Lambda(1405)$ by regarding it as the two-pole structure of the resonance.

Another resonance $\Lambda(1520) \equiv \Lambda^*$ attracts also a great deal of attention. This resonance of $J^P = 3/2^-$ is well established with a relatively narrow decay width $\Gamma \sim 15$ MeV. In the quark model it is a member of 70-plet of SU(6) with $l = 1$ excitation, and is mostly dominated by the flavor singlet component. In the dynamical treatment of meson-baryon scattering, it appears as a quasibound state of π and $\Sigma(1385)$. Both methods are equally successful in explaining the currently existing data of the Λ^*. However, they have a very different structure in its wave function and make different predictions in some physical quantities.

In modern experimental facilities such as the SPring-8 and Jefferson Laboratory (JLab), production experiments of this resonance can be carried out with high precision, so that it is of great interest and importance to study the reactions theoretically. Understanding the mechanism of the Λ^* production is very useful not only for the extraction of its properties but also for the explanation of the recent observation of the peak structure corresponding to the Θ^+ in the reaction $\gamma + d \to \Theta^+ + \Lambda^*$. Motivated by these facts, there have been several works on this reaction both experimentally [1] and theoretically [2–4] recently.

In addition to the previous experiments for the Λ^* photoproduction [5,6], a recent experiment conducted by the LEPS Collaboration at the SPring-8 revealed an interesting feature: It turned out that the production rate of the Λ^* was strongly dependent on the target nucleon, which implies that the production mechanism of the Λ^* photoproduction has strong charge asymmetry. Interestingly, this feature is consistent with the theoretical prediction of Ref. [3] in which it was proposed that this asymmetry might be explained by the contact term, which was required in order to satisfy the gauge invariance and was present for the proton target ($\gamma p \to K^+\Lambda^*$) but not for the neutron target ($\gamma n \to K^0\Lambda^*$). The size of the contact term is significant, at least as compared with the s channel, u channel, and kaon exchange in the t-channel process. The contact-term dominance shown in the previous study [3], however, depends on the unknown strength of the K^*-exchange diagram which is active both for the proton and neutron in the almost same order of magnitude. The importance of the contact term was ignored in the analysis of the previous experiments [5,6], while the role of the K^* exchange was emphasized.

It is now of great importance to test each contribution of various terms in the reaction, especially that of the contact and K^*-exchange terms. In the present work, we aim at investigating this issue in detail. In the current and future experiments such as the LEPS and the CLAS at the JLAB, various angular distributions are expected to be available with the polarized photon and nucleon target utilized. Therefore, we consider the differential cross sections under different conditions of the polarization of the beam and target so that we may extract information on how each term contributes to the differential cross sections.

This paper is organized as follows: In Sec. II, we explain the present method briefly. We define various effective interactions which are necessary to compute the transition amplitudes. In Sec. III, we present the differential cross

*Electronic address: sinam@pusan.ac.kr
†Electronic address: kschoi@pusan.ac.kr
‡Electronic address: hosaka@rcnp.osaka-u.ac.jp
§Electronic address: hchkim@pusan.ac.kr

sections with each Born diagram separately, including the s-, u-, t-channel processes and contact term. In Sec. IV, we consider possible experimental conditions to distinguish the contact-term dominance from K and K^* exchanges by using angular distributions and asymmetries. The final section is devoted to summary and conclusions.

II. EFFECTIVE LAGRANGIAN METHOD

In this section we define the effective Lagrangians relevant to the $\gamma p \to K^+\Lambda^*$ process as depicted in Fig. 1, where we consider five tree (Born) diagrams: s channel (upper left), u channel (upper right), t channel with pseudoscalar K^- exchange [$t(p)$] and with vector K^{*-} exchange [$t(v)$] (lower left), and contact term (lower right). We define the momenta of the photon, pseudoscalar kaon, vector kaon, nucleon, and Λ^* as shown in Fig. 1. The spin-3/2 particle is treated as a Rarita-Schwinger field [7–9], and its treatment can be found in Ref. [3] in detail. The relevant effective Lagrangians are then given as follows:

$$
\begin{aligned}
\mathcal{L}_{\gamma NN} &= -e\bar{N}\left(\not{A} + \frac{\kappa_N}{4M_p}\sigma_{\mu\nu}F^{\mu\nu}\right)N + \text{H.c.},\\
\mathcal{L}_{\gamma KK} &= ie\{(\partial^\mu K^\dagger)K - (\partial^\mu K)K^\dagger\}A_\mu,\\
\mathcal{L}_{\gamma\Lambda^*\Lambda^*} &= -e\bar{\Lambda}^{*\mu}\left(\not{A} + \frac{\kappa_{\Lambda^*}}{4M_{\Lambda^*}}\sigma_{\nu\rho}F^{\nu\rho}\right)\Lambda^*_\mu + \text{H.c.},\\
\mathcal{L}_{\gamma KK^*} &= g_{\gamma KK^*}\epsilon_{\mu\nu\sigma\rho}(\partial^\mu A^\nu)(\partial^\sigma K)K^{*\rho} + \text{H.c.},\\
\mathcal{L}_{KN\Lambda^*} &= \frac{g_{KN\Lambda^*}}{M_K}\bar{\Lambda}^{*\mu}\Theta_{\mu\nu}(A, Z)(\partial^\nu K)\gamma_5 p + \text{H.c.},\\
\mathcal{L}_{K^*N\Lambda^*} &= -\frac{ig_{K^*N\Lambda^*}}{M_{K^*}}\bar{\Lambda}^{*\mu}\gamma^\nu(\partial_\mu K^*_\nu - \partial_\nu K^*_\mu)p + \text{H.c.},\\
\mathcal{L}_{\gamma KN\Lambda^*} &= -i\frac{eg_{KN\Lambda^*}}{M_K}\bar{\Lambda}^{*\mu}A_\mu K\gamma_5 N + \text{H.c.},
\end{aligned}
\tag{1}
$$

where N, Λ^*_μ, K, K^*, and A^μ are the nucleon, Λ^*, pseudoscalar kaon, vector K^*, and photon fields, respectively. $\Theta_{\mu\nu}$ stands for the off-shell effect [3]. The interaction for the $K^*N\Lambda^*$ vertex is taken from Ref. [10]. As for the $\gamma\Lambda^*\Lambda^*$ vertex for the u channel, we utilize the effective interaction suggested by Ref. [11] which contains four form factors of different multipoles. We ignore the electric coupling F_1, since the Λ^* is neutral. We also neglect F_3 and F_4 terms, assuming that higher multipole terms are less

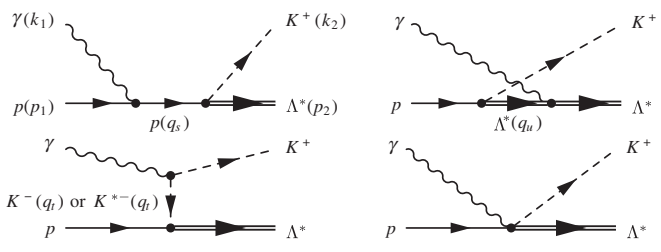

FIG. 1. The relevant diagrams for the Λ^* photoproduction.

important. Hence, for the photon coupling to the Λ^*, we consider only the magnetic coupling term F_2 whose strength is proportional to the anomalous magnetic moment of the Λ^*, κ_{Λ^*}. In the present work, we set $\kappa_{\Lambda^*} = 1$ as a trial. We will see that the u-channel contribution is very small as compared to the dominant contact term if the κ_{Λ^*} is not too large. The $KN\Lambda^*$ coupling constant, $g_{KN\Lambda^*}$ is determined to be 11 by using the experimental data ($\Gamma_{\Lambda^*\to\bar{K}N} = 15.6 \times 45\%$ MeV) [12]. We will discuss the $K^*N\Lambda^*$ coupling constant shortly. We note that the last Lagrangian in Eq. (1) represents the contact-term interaction which is necessary to maintain the Ward-Takahashi identity of the amplitudes.

Having set up these Lagrangians, we can write the scattering amplitudes as follows:

$$
\begin{aligned}
i\mathcal{M}_s &= -\frac{eg_{KN\Lambda^*}}{M_K}\bar{u}^\mu(p_2, s_2)k_{2\mu}\gamma_5\frac{(\not{p}_1 + M_p)F_c + \not{k}_1 F_s}{q_s^2 - M_p^2}\\
&\quad\times \not{\epsilon}u(p_1, s_1) + \frac{e\kappa_p g_{KN\Lambda^*}}{2M_pM_K}\bar{u}^\mu(p_2, s_2)k_{2\mu}\gamma_5\\
&\quad\times\frac{(\not{q}_s + M_p)F_s}{q_s^2 - M_p^2}\not{\epsilon}\not{k}_1 u(p_1, s_1)\\
i\mathcal{M}_u &= -\frac{g_{KN\lambda}\kappa_{\Lambda^*}}{2M_KM_\Lambda}\bar{u}_\mu(p_2)\not{k}_1\not{\epsilon}D^\mu_\sigma\Theta^{\sigma\rho}k_{2\rho}\gamma_5 u(p_1)F_u,\\
\mathcal{M}_t &= \frac{2eg_{KN\Lambda^*}}{M_K}\bar{u}^\mu(p_2, s_2)\frac{q_{t,\mu}k_2\cdot\epsilon}{q_t^2 - M_K^2}\gamma_5 u(p_1, s_1)F_c,\\
i\mathcal{M}_c &= \frac{eg_{KN\Lambda^*}}{M_K}\bar{u}^\mu(p_2, s_2)\epsilon_\mu\gamma_5 u(p_1, s_1)F_c,\\
i\mathcal{M}_v &= \frac{-ig_{\gamma KK^*}g_{K^*NB}}{M_{K^*}(q_t^2 - M_{K^*}^2)}\bar{u}^\mu(p_2, s_2)\gamma_\nu(q_t^\mu g^{\nu\sigma} - g_t^\nu q^{\mu\sigma})\\
&\quad\times\epsilon_{\rho\eta\xi\sigma}k_1^\rho\epsilon^\eta k_2^\xi u(p_1, s_1)F_v,
\end{aligned}
\tag{2}
$$

where ϵ and u^μ are the photon polarization vector and the Rarita-Schwinger vector-spinor. Here, we set $\Theta_{\mu\nu} = g_{\mu\nu}$ for simplicity. $D_{\mu\nu}$ is the spin-3/2 fermion propagator [3,13], for which here we use the usual spin-1/2 fermion propagator, since the difference is negligible in the relatively low-energy regions [3]. For the form factor, we employ the gauge-invariant one with the four momentum cutoff Λ, which was used for the study of $\gamma N \to K\Lambda^*$ in Ref. [3]:

$$
\begin{aligned}
F_x(q^2) &= \frac{\Lambda^4}{\Lambda^4 + (x - M_x^2)^2}, \qquad x = s, u, t(p), t(v),\\
F_c &= F_s + F_u - F_sF_u.
\end{aligned}
\tag{3}
$$

Here M_x is the on shell mass of the exchange particle in the x channel. In Ref. [3], it was shown that the use of this form factor in Eq. (3) satisfies the Ward-Takahashi identity and can reproduce the existing data qualitatively well.

In the present treatment there are two unknown parameters, i.e. the cutoff Λ in the form factor and the $K^*N\Lambda^*$ coupling constant. The former is fixed to be $\Lambda = 700$ MeV as done in Refs [3,14]. The only remaining unknown is the

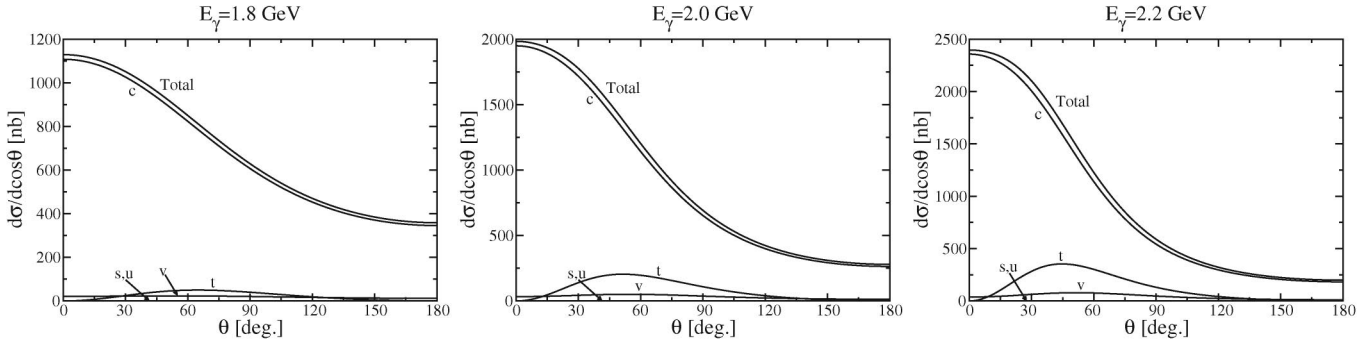

FIG. 2. Each contribution to the differential cross sections as a function of θ at three different photon energies $E_\gamma = 1.8$, 2.0, and 2.2 GeV and the differential cross section with all contributions. The c, s, u, and v denote the contact term, the s channel, the u channel, and K^* exchange, respectively.

strength of the $K^*N\Lambda^*$ coupling constant. In theoretical models, the coupling constant is rather small [15]. Since this value affects the feature of the contact-term dominance, we will treat it as a free parameter and see how much the contact term contributes to the amplitude.

III. RESULTS AND DISCUSSION

A. Dominant processes

In Ref. [3], it was already shown that the contribution of the contact term was significantly larger than those from the s, u, t channels and K^* exchange when $|g_{K^*N\Lambda^*}|$ was not too large, i.e. $|g_{K^*N\Lambda^*}| \lesssim 10$. In order to verify it, we need to examine each contribution to the differential cross sections in detail.

In Fig. 2, we draw the differential cross sections for each contribution separately as well as that with all contributions as functions of the scattering angle θ of the kaon at three different photon energies, $E_\gamma = 1.8$, 2.0, and 2.2 GeV, respectively. The $K^*N\Lambda^*$ coupling constant is fixed to be $g_{K^*N\Lambda^*} = 11$ for K exchange. We observe from Fig. 2 that the differential cross section with all contributions increase, in particular, in the forward direction as E_γ increases. As shown in Fig. 2, the contact term is the most dominant one that makes almost all contributions to the differential cross section, even though the sizes of the K- and K^*-exchange contributions are still nonnegligible. On the contrary, those of the s and u channels turn out to be tiny. Therefore, it is sufficient to consider the contact term, K and K^* exchanges.

B. ϕ dependence with polarized photon beams

It is of great interest to determine which particle is exchanged in the course of the photoproduction. In fact, it is possible to pinpoint the exchange particle if the photon beam can be polarized in various ways. In this case, the dependence on the azimuthal angle (ϕ) becomes important in addition to the scattering angle. In order to study the dependence of each channel on the ϕ, we take the z axis for the incident photon beam, the x axis for the scattering plane, and the y axis to be perpendicular to the scattering plane (see Fig. 3). If we take a linearly polarized photon, then the ϕ can be defined as that between the photon polarization and the x axis.

Let us first show how different ϕ dependence emerges according to the type of the electromagnetic interaction. This is particularly useful to distinguish one type from the other in meson exchange diagrams of the t channel. Consider the K-exchange amplitude which contains the γKK coupling constant. The coupling constant is an electric type and has the following structure: $\boldsymbol{\epsilon} \cdot (\vec{q} + \vec{p}_f)$, where $\vec{q}$ and $\vec{p}_f$ are the momenta of the exchanged (intermediate) and final-state kaons. Therefore, the scattered kaon and nucleon in the final state are produced most likely to be in the direction parallel to the photon polarization vector. Explicitly, the resulting ϕ dependence of the cross section is proportional to $\cos^2\phi$, as shown in Fig. 4. For K^* exchange, there are several terms for the γKK^*, but the important piece has a structure of the magnetic type, i.e. $\vec{\epsilon} \times \vec{q} \cdot \vec{p}_f$. Hence, the final-state kaon and nucleon are produced most likely in the direction perpendicular to the photon polarization, which is proportional to $\sin^2\phi$. This behavior also can be verified as shown in Fig. 4, although it is not exactly $\sin^2\phi$. Different angular distributions depending on which particle is exchanged was used in the analysis of the ϕ photoproduction and in the study of $\Lambda(1405)$ photoproduction. As compared to the t-channel

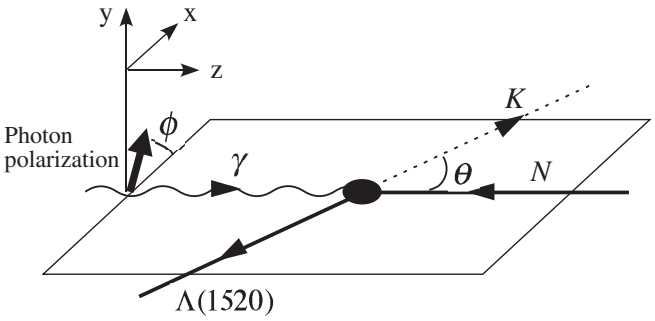

FIG. 3. Definition of axes on the reaction plane and scattering and azimuthal angles θ and ϕ.

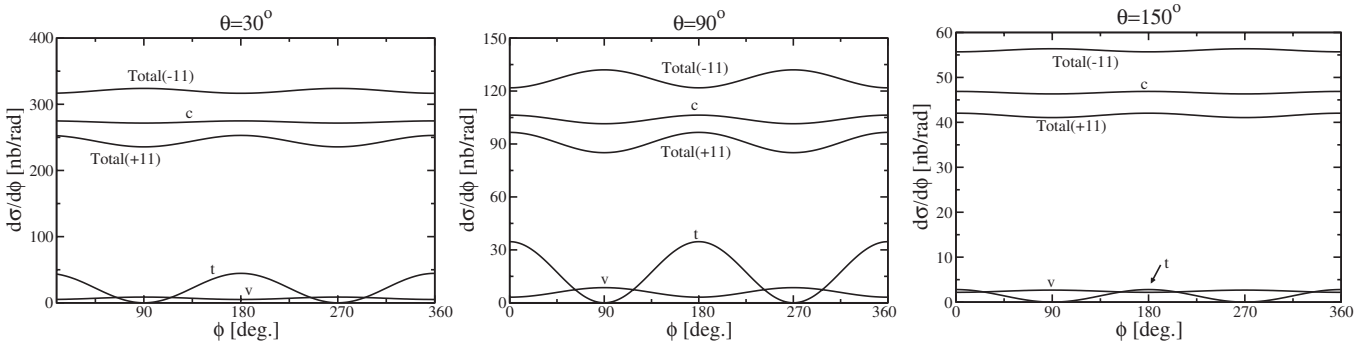

FIG. 4. Each contribution to the differential cross sections as a function of ϕ at three different scattering angles $\theta = 30°$, $90°$, and $150°$. The photon energy is fixed to be $E_\gamma = 2$ GeV, and $g_{K^*N\Lambda^*} = \pm 11$. The c, t, and v denote the contact term, the t channel, and K^* exchange, respectively.

processes, the ϕ dependence is not so strong for the contact term.

As an alternative method instead of the ϕ dependence, it is also convenient to consider the asymmetry defined as

$$A(E_\gamma, \theta) = \frac{(\frac{d\sigma}{d\theta})_\perp - (\frac{d\sigma}{d\theta})_\parallel}{(\frac{d\sigma}{d\theta})_\perp + (\frac{d\sigma}{d\theta})_\parallel}. \tag{4}$$

The subscripts $\parallel$ and $\perp$ in Eq. (4) stand for the direction of the photon polarization vectors parallel and perpendicular to the reaction plane, respectively. The asymmetry integrated over the scattering angle is then defined as:

$$A(E_\gamma) = \frac{1}{2}\int A(E_\gamma, \theta)\sin\theta d\theta. \tag{5}$$

Coefficient $1/2$ on the right-hand side is introduced for the normalization of $A(E_\gamma)$ such that it reduces to either 1 or -1 when $(d\sigma/d\theta)_\perp$ or $(d\sigma/d\theta)_\parallel$ vanishes.

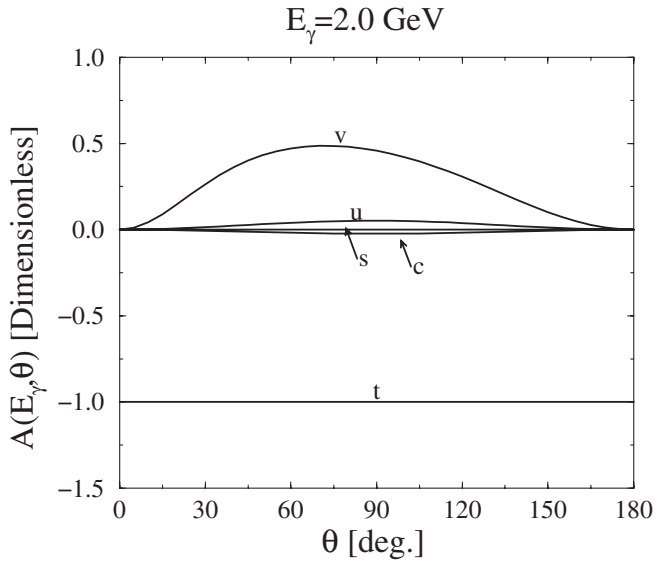

FIG. 5. Asymmetry $A(E_\gamma, \theta)$ for various contributions.

In Fig. 5, $A(E_\gamma, \theta)$ is depicted as a function of θ for various terms separately at the photon energy 2.0 GeV. Since the s, u channels and contact term show weak ϕ dependence for the whole range of θ, the asymmetry turns out to be almost zero, while the K-exchange asymmetry has $A(E_\gamma, \theta) = -1$, which follows from the fact that the cross section vanishes at $\phi = 0$. In contrast, $A(E_\gamma, \theta)$ of K^* exchange takes positive values except for $\theta = 0$ and π, which is due to the magnetic type coupling, though not complete. Therefore, we have established a characteristic difference in three dominant terms: $A(E_\gamma, \theta) \sim 0$ for the contact term, $A(E_\gamma, \theta) = -1$ for the K exchange one, and $A(E_\gamma, \theta) \lesssim 0$ for the K^* exchange one. In Fig. 6, we show the asymmetries $A(E_\gamma, \theta)$ for the proton target ($\gamma p \to K^+\Lambda^*$) with all diagrams included as functions of θ and at different photon energies (upper-left, upper-right, and lower-left panels). Also shown is the θ-integrated $A(E_\gamma)$ as a function of E_γ (lower-right panel). We observe that in general the asymmetry is small due to the presence of the contact term. As the strength of the $K^*N\Lambda^*$ coupling constant is increased, the asymmetry takes finite values either of positive (for the positive $K^*N\Lambda^*$ coupling constant) or of negative value (for negative $K^*N\Lambda^*$ coupling constant).

Although it is experimentally more difficult to perform such a test in the neutron reaction ($\gamma n \to K^0\Lambda^*$), K^* exchange becomes important without the contact and K-exchange terms. The asymmetry, therefore, is expected to be positive in this case.

C. Polarized target

If the target nucleon is polarized and at the same time if it is possible to measure the polarization of Λ^*, we can check a consistency for the spin of the produced particle [$\Lambda(1520)$] owing to the conservation of its helicity. Although it is probably a very difficult situation experimentally, we would like to see what may be expected in observation.

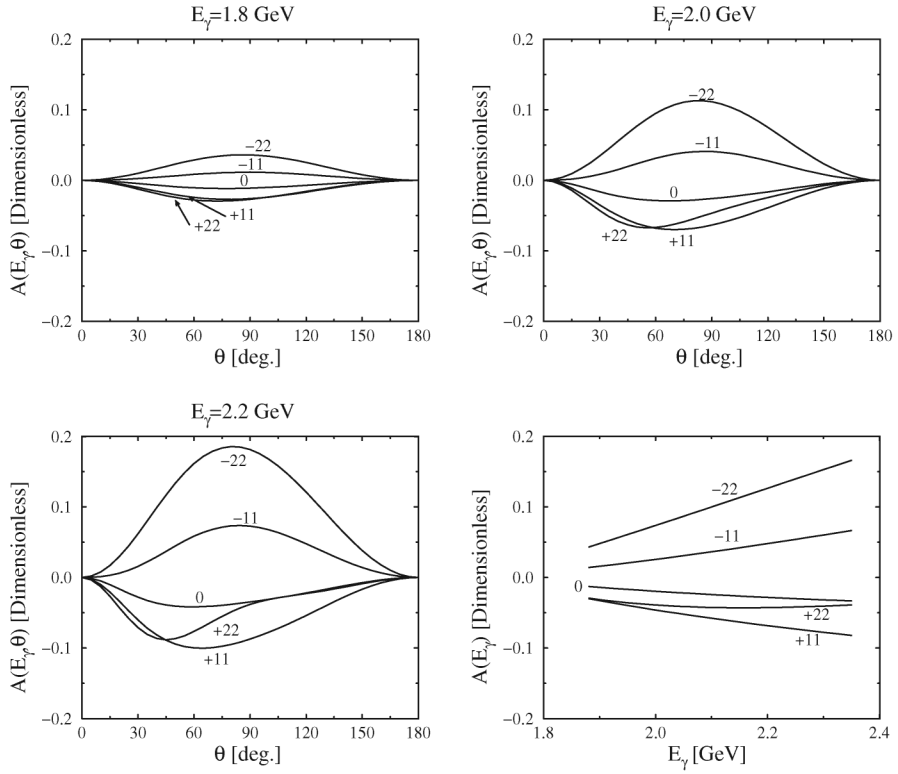

FIG. 6. Asymmetry $A(E_\gamma, \theta)$ for the different photon energies, $E_\gamma = 1.8$ (upper left), 2.0 (upper right), and 2.2 GeV (lower left). $A(E_\gamma)$ of Eq. (5) is shown in the lower-right panel. The labels on the figure denote the values of the $K^*N\Lambda^*$ coupling constant.

Suppose that we set the spin of the target proton to be $S_z(p) = +1/2$ and the photon polarization $S_z(\gamma) = +1$. Then the total helicity is $3/2$. In the forward angle scattering, the z component of the total angular momentum is carried solely by the helicity. Hence, the forward cross section can take a finite value when the spin of $\Lambda(1520)$ is $S_z(\Lambda^*) = +3/2$. Otherwise, it vanishes. This is a simple selection rule, but may be helpful for some reactions. For instance, for the $\Lambda(1116)$ production, since it has spin-1/2, the forward production under the above condition, i.e. $S_z(p) = +1/2$ and $S_z(\gamma) = +1$, cannot occur. As the scattering angle θ increases, however, the cross section becomes finite.

To see this situation explicitly, we show in Fig. 7 the differential cross sections for the polarized target $S_z(p) = +1/2$, the polarization of the final $\Lambda(1520)$ being either $S_z(\Lambda^*) = +3/2$ or $-3/2$. The case of $S_z(\Lambda^*) = +3/2$ is allowed while the other is suppressed, which is clearly seen in Fig. 7. In this particular example, it is interesting to see not only that the differential cross section for $S_z(\Lambda^*) = -3/2$ becomes exactly zero at $\theta = 0$ and π but also that the magnitudes of these two cases are very much different:

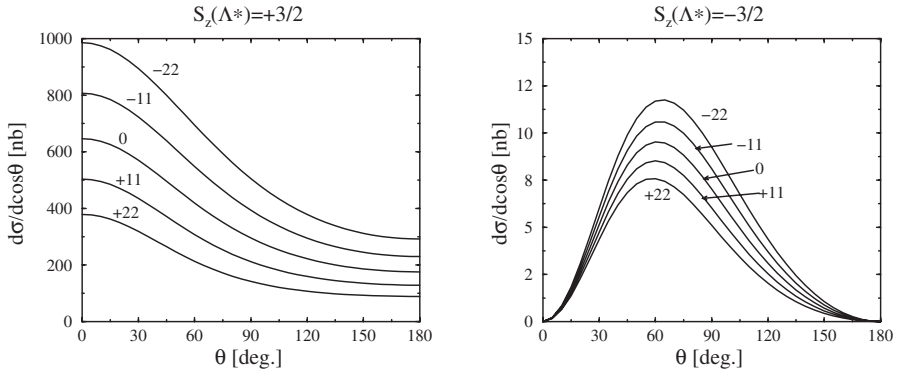

FIG. 7. The differential cross section of the reaction $\gamma p \to K^+\Lambda^*$ with the polarized target at $E_\gamma = 1.8$ GeV. The labels on the figure denote the values of the $K^*N\Lambda^*$ coupling constant.

The suppressed differential cross section is very much smaller than the allowed one by more than 2 orders of magnitude.

D. Some implications to Θ^+ photoproduction

One of the motivations of the present work is to apply the reaction mechanism which can be established for the known resonance $\Lambda(1520)$ to reactions involving Θ^+. In fact, assuming that the spin and parity of Θ^+ are the same as those of $\Lambda(1520)$, $J^P = 3/2^-$, we can apply the present results almost straightforwardly to the case of Θ^+ within the framework of the effective Lagrangian approach. For example, we have already reported a large asymmetry between the cross sections of the proton and neutron targets [16]. The reaction rate of charge exchange process is significantly larger than that of charge nonexchange process. For the case of $\Lambda(1520)$ the proton target reaction is larger, while it is the other way around for the case of Θ^+, that is, the neutron target reaction is dominant.

In drawing this conclusion, however, it is crucial to know the strength of the $K^*N\Theta^+$ coupling constant, since the K^*-exchange process does not have a strong selectivity between the proton and neutron target reactions. As discussed in Refs. [16,17], the K^*-exchange process plays an important role in angular distributions as well as in determining the magnitude for the cross sections. For the case of $\Lambda(1520)$, a recent study indicates that the coupling is not very strong and the above feature is maintained [15]. On the contrary, the $K^*N\Theta^+$ coupling constant is not known, but a naïve estimation in the quark model is not so strong, and therefore the above feature of charge exchange dominance is not very much affected.

We consider that the measurement and comparison of the experimental and theoretical values of the $K^*N\Lambda^*$ coupling constant is important, in order to test the applicability of the presently available models for hadrons, especially in the kaon productions. Once they are established, we also can extend the same method to the physics of exotic hadrons including the Θ^+, particularly because the energies of the $\Lambda(1520)$ and Θ^+ reactions are expected to be very similar. Such a strategy should be of great use in order to understand the structure of exotic hadrons. Once again, as shown in Fig. 2, the different ϕ dependence is helpful to determine the value for $g_{K^*N\Theta}$. We would like to emphasize also that the discussion of ϕ dependence is applied to the resonance productions of spin-1/2.

Another feature of the helicity conservation also can be applied to the Θ^+ productions. Just as in the case of $\Lambda(1520)$, this will help us make some constraints on the unknown spin of the Θ^+.

IV. SUMMARY AND CONCLUSIONS

In the present work, we have investigated the $\gamma N \to K^+\Lambda^*$ reaction in the effective Lagrangian approach. In particular, we aim at scrutinizing each contribution of various diagrams to the reaction: On one hand, the contact term plays the crucial role in describing the $\gamma p \to K^+\Lambda^*$ process. On the other hand, the K^*-exchange term may become nonnegligible. It is of utmost importance to understand this difference, since the contact term exists in the proton channel while it is absent in the neutron channel, so that the rate of the Λ^* production turns out to be suppressed in the neutron target.

We have asserted that it is of great use to investigate the azimuthal angular distributions of the differential cross section in order to understand the role of each contribution. In particular, the angular ϕ distribution, or alternatively, the asymmetries $A(E_\gamma, \theta)$ and $A(E_\gamma)$, which can be measured by using the polarized photon beam, distinguish each role of the contact term, K^*-exchange, and K-exchange terms according to the polarization of the photon beam. We have observed that if the contact term dominates, the asymmetry becomes almost zero, while the K^*-exchange contribution increases, the asymmetry becomes finite. Hence, a measurement of the asymmetries will provide a touchstone for understanding the reaction mechanism of the Λ^* photoproduction.

Not only theoretically but also experimentally, the contact-term dominance is one of the most interesting features for the spin-3/2 baryon photoproduction as well as for the Λ^* photoproduction in general. In spite of possible model dependence in treating baryons with different spins, the above-mentioned feature does not appear in the spin-1/2 baryon photoproduction. An experimental confirmation of the contact-term dominance in the Λ^* photoproduction is important and may be a challenging task. As discussed in the present work, since the test of the contact-term dominance can be made, in particular, in the very forward direction and near the threshold, the LEPS Collaboration at the SPring-8 may be one of the good places for verifying it.

ACKNOWLEDGMENTS

The present work is supported by the Korea Research Foundation Grant funded by the Korean Government (MOEHRD) (KRF-2006-312-C00507). We are grateful to T. Nakano and A. Titov for fruitful discussions. S. i. N. would like to thank K. Horie, S. Shimizu, J. K. Ahn, T. Hyodo, and T. Sawada for interesting and stimulating discussions about this work. S. i. N. also appreciates the hospitality during his stay at RCNP in Japan, where part of this work was performed. The work of A. H. is supported in part by the Grant for Scientific Research [(C) No. 16540252] from the Education, Culture, Science and Technology of Japan. The work of S. i. N. is supported in part by the Brain Korea 21 (BK21) project in Center of Excellency for Developing Physics Researchers of Pusan National University, Korea.

[1] T. Nakano, Int. J. Mod. Phys. A **20**, 1543 (2005).
[2] L. Roca, E. Oset, and H. Toki, hep-ph/0411155.
[3] S. i. Nam, A. Hosaka, and H.-Ch. Kim, Phys. Rev. D **71**, 114012 (2005).
[4] A. I. Titov, B. Kampfer, S. Date, and Y. Ohashi, Phys. Rev. C **72**, 035206 (2005); **72**, 049901 (2005).
[5] A. Boyarski, R. E. Diebold, S. D. Ecklund, G. E. Fischer, Y. Murata, B. Richter, and M. Sands, Phys. Lett. **34B**, 547 (1971).
[6] D. P. Barber *et al.*, Z. Phys. C **7**, 17 (1980).
[7] W. Rarita and J. S. Schwinger, Phys. Rev. **60**, 61 (1941).
[8] L. M. Nath, B. Etemadi, and J. D. Kimel, Phys. Rev. D **3**, 2153 (1971).
[9] C. R. Hagen, Phys. Rev. D **4**, 2204 (1971).
[10] R. Machleidt, K. Holinde, and C. Elster, Phys. Rep. **149**, 1 (1987).
[11] M. Gourdin, Nuovo Cimento **36**, 129 (1965); **40A**, 225 (1965).
[12] W. M. Yao *et al.* (Particle Data Group), J. Phys. G **33**, 1 (2006).
[13] B. J. Read, Nucl. Phys. **B52**, 565 (1973).
[14] S. i. Nam, A. Hosaka, and H.-Ch. Kim, Phys. Rev. D **70**, 114027 (2004).
[15] T. Hyodo, S. Sarkar, A. Hosaka, and E. Oset, Phys. Rev. C **73**, 035209 (2006).
[16] S. i. Nam, A. Hosaka, and H.-Ch. Kim, Phys. Lett. B **633**, 483 (2006).
[17] S. i. Nam, A. Hosaka, and H.-Ch. Kim, Phys. Rev. C **74**, 025204 (2006).